Nuclear localization of nm23-h1 in head and neck squamous cell carcinoma is associated with radiation resistance

Haeng Ran Park

Department of Medical Science

The Graduate School, Yonsei University

Nuclear localization of nm23-h1 in head and neck squamous cell carcinoma is associated with radiation resistance

Directed by Professor Nam Hoon Cho

The Master's Thesis
Submitted to the Department of Medical Science,
the Graduate School of Yonsei University
in partial fulfillment of the requirements for the degree
of Master of Medical Science

Haeng Ran Park

June 2011

This cerifies that Master's Thesis

of Haeng Ran Park is approved

Thesis Supervisor : Nam Hoon Cho

Thesis Committee Member : Se-Heon Kim

Thesis Committee Member : Jaeho Cho

The Graduate School

Yonsei University

June 2011

ACKNOWLEDGEMENTS

2년의 석사 학위 과정을 보내면서 그 시간들을 다시 한번 돌이켜보게 되는데, 힘든 시간보다 재미있고 즐거웠던 일들이 먼저 떠오르면서 미소를 짓게 합니다. 실험이라는 것을 전혀 몰랐던 내가 여기서 하나하나 배우고 그 배운걸 토대로 실험해서 나온 결과가 신기하기만 했었고, 많은 실수와 실패를 거치면서 만들어진 데이터로 하나의 스토리를 만들어 갈 때 논문은 이렇게 해서 만들어지는구나 라고 느끼게 했던 시간들이었습니다. 필요한 정보들을 혼자서 찾는 연습을 하면서 여러가지 방법과 길이 있다는 것을 알 수 있었고, 하나하나 이루는 습관을 들인 것 같아 너무나 큰 도움이 되었던 시간이었습니다. 학위 과정을 하는 동안이 저에게는 더 없이 귀중한 재산으로 남을 것 같습니다.

본 연구를 수행하는데 있어서 아낌없는 지도와 조언으로 이끌어 주시며 연구에 대한 뜨거운 열정으로 귀감이 되시는 조남훈 교수님께 진심으로 감사드립니다. 바쁘신 와중에도 항상 귀중한 시간을 내시어 소중한 가르침을 주셨고, 실험 진행이 잘 되지 않을 때 충분히 수행해 낼 수 있다는 믿음을 심어주셨습니다. 항상 격려해 주시고 바른 길로 인도해주시며, 연구를 위해 물심양면 지원을 아끼지 않으신 김세헌 교수님께 이 자리를 빌어 다시 한번 감사 드립니다. 바쁘신 와중에도 항상 챙겨주시며 신경써 주셔서 감사드립니다. 바쁘신 와중에도 저의 미흡한 논문을 심사하시느라 귀한 시간을 내어주시고 많은 조언과 지도해주신 조재호 교수님께 진심으로 감사 드립니다. 멋지고도 항상 우리랩을 챙겨주시며 실험적 조언을 아낌없이 주신 강숙희 선생님, 같이 학위 과정을 보내면서 도와주고 믿어주었던 김백길 선생님, 최윤표 선생님, 고명청 선생님, 강규섭 선생님께 이 자리를 빌어 감사의 말을 전합니다.

무엇보다 이 학위를 무사히 마칠 수 있도록 한결 같은 마음으로 지켜봐 주고 염려와 격려해 준 가족들 친구들 모두에게 감사 드립니다.

June, 2011
Haeng Ran Park

TABLE OF CONTENTS

LIST OF FIGURES

LIST OF TABLES

Abstract

Nuclear localization of Nm23-h1
in head and neck squamous cell carcinoma is associated
with radiation resistance

Haeng Ran Park

Department of Medical Science

The Graduate School, Yonsei University

(Directed by Professor Nam Hoon Cho)

Background: Although radiation resistance is a primary issue in radiation therapy, attempts to find predictors of radiation resistance have met with little success. The authors therefore aimed to determine predictors for to improve the prognosis of head and neck squamous cell carcinoma (HNSCC).

Methods: HNSCC cell lines, SCC15, SCC25, and QLL1, irradiated with an acute dose of 4 Gy (RR-4), a cumulative dose of 60 Gy (RR-60), and a booster dose of 4 Gy over 60 Gy (RR-60+4), were used with nonirradiated cell lines. Those were used in cDNA microarray, proteomics, western blotting, and immunofluorescence, respectively. One hundred five HNSCC tissue samples with radiation resistance were analyzed by immunohistochemistry.

Results: Western blot analysis of RR-60 cell lines was identical to the data of Nm23-H1 overexpression by cDNA array and proteomic screening. Immunofluorescence demonstrated significant nuclear translocation of Nm23-H1 in

RR-4 and RR-60 cell lines, and less but still intense nuclear shuttling in RR-60+4. Similarly, Nm23-H1 nuclear localization was observed in 20% (21/105) of tissue samples. Univariate analysis demonstrated that Nm23-H1 nuclear localization was strongly associated with overall and recurrence-free survival. Multivariate stepwise Cox regression analysis showed that Nm23-H1 nuclear localization (odds ratio [OR], 7.48) and N stage (OR, 2.13) were associated with overall survival, and Nm23-H1 nuclear localization (OR, 3.02), T stage (OR, 1.43), and insufficient tumor margin (OR, 3.27) were associated with recurrence-free survival.

Conclusion: Overexpression of Nm23-H1, specifically its nuclear translocation, may be powerful predictor of RR in HNSCC.

Keywords: Nm23-H1, nuclear localization, radiation resistance, head and neck squamous cell carcinoma, predictor

Nuclear localization of Nm23-h1
in head and neck squamous cell carcinoma is associated
with radiation resistance

Haeng Ran Park

Department of Medical Science

The Graduate School, Yonsei University

(Directed by Professor Nam Hoon Cho)

I. INTRODUCTION

Radiation resistance (RR) is clinically presented as locoregional failure and a serious problem for patients with advanced head and neck squamous cell carcinoma (HNSCC). RR is responsible in part for 5-year survival rates below 50% of patients with HNSCC. [1] Many attempts have been made to enhance the effectiveness of radiation therapy, including altered fractional schemes, incorporation of chemotherapy, and molecular targeted therapy. However, despite the development of anti-epithelial growth factor receptor (EGFR) immunotherapy, small molecule kinase inhibitors, and adenoviral vectors to restore p53 or re-express p16,[2] surgery and radiotherapy remain the preferred treatments for primary HNSCC.

Despite vigorous trials to discover biomarkers that predict RR, there have been few surrogate target markers, probably not only because the majority of candidates have dependented on the exiting methods, but also because they have not been validated in clinical practice. However, biomarkers for the prediction of RR are urgently needed to improve disease-free and overall survival of patients with

advanced cancers, including HNSCC. In fact, cellular radiosensitivity is the result of a combinatorial process comprising a wide variety of signaling and effector molecules. For instance, effects of EGFR function on radiosensitivity have been suggested, but the role of EGFR in radiosensitivity remains controversial.[3-5] In addition, Bcl-2 overexpression and p53 mutation were also associated with RR in HNSCC.[6] PI3K activation, as assessed by Akt phosphorylation, or overexpression of hypoxia-inducible factors (e.g., HIF1a and carbonic anhydrase 9) may predict RR in tumors showing locoregional failure.[7, 8] Excision repair cross-complementation group 1 (ERCC1) has also been demonstrated to predict poor survival,[9] and hedgehog activation has been reported to contribute to chemoradiation resistance in patients with esophageal cancer with RR.[10]

We focused on Nm23-H1 as a biological predictor of RR based on both cDNA array and proteomics in the present study. Nm23-H1 is a ubiquitously distributed nuclear diphosphate kinase (NDP) that catalyzes the phosphorylation of nucleoside diphosphates.[11] During tumor metastasis, Nm23-H1 may inhibit motility in response to serum and platelet-derived growth factors,[12] reduce ERK activation in response to signaling,[13, 14] and disassemble the cytoskeleton.[15, 16] In the present study, we established radiation-resistant cell lines with cumulative irradiation dosages identical to the amounts administered in radiotherapy for patients with HNSCC, and retrospectively analyzed HNSCC patients tissue samples with RR. In addition, the biological properties of Nm23-H1 were assessed to characterize RR in the event of Nm23-H1 nuclear localization.

II. MATERIALS AND METHODS

1. Generation of radiation-resistant cell lines

HNSCC cell lines, SCC15, SCC25, and QLL1, were cultured in Minimum Essential Media (MEM; GIBCO-BRL, Gaithersburg, MD, USA) supplemented with 10% fetal bovine serum (FBS; GIBCO-BRL), and 1% penicillin and 1% streptomycin. Renal cell carcinoma cell line, Caki-1, used for the acute 4 Gy dose irradiation (RR-4) test, was maintained in RPMI1640 (GIBCO-BRL) with 10% FBS and 1% antibiotics. All cell lines were maintained at 37°C in a humidified atmosphere of 5% CO_2.

Cells initially treated with 2 Gy radiation were grown to 80% confluence after seeding into another flask, and aliquots accumulated a dosage of 60 Gy after 30 repetitions. Those cells were characterized as radiation-resistant to the cumulative dose of 60 Gy (RR-60), with subsequent radiation of 4Gy (RR- 60+4).

2. cDNA array

All procedures from RNA extraction to cDNA microarray data analysis were done as previously described. [17]

The only difference between our study and previous ones is that non-irradiated cell lines RNA were labeled with cy3.

Proteomics

3. Protein Extraction

Both RR-60 and non-irradiated cells were directly homogenized with a motor-driven homogenizer (PowerGen125, Fisher Scientific) in two-dimensional gel electrophoresis (2-DE) lysis solution composed of 7 M urea, 2 M thiourea, 4% (w/v) 3-[(3-cholamidopropyl) dimethylammonio]-1-propanesulfonate (CHAPS), 1% (w/v) dithiothreitol (DTT), 2% (v/v) pharmalyte, and 1 mM benzamidine. Proteins were extracted by vortexing for 1hr and centrifugation at 15,000*g* for 1hr at 15°C. Insoluble materials were discarded, and the soluble fractions were saved for 2-DE. Protein concentration was measured by Bradford assay.

4. 2-DE and Image Analysis

Briefly, 200 μg of protein extract was separated by IEF using an IPG strip with a nonlinear pH gradient of 4 to 10 (Genomine Inc., Kyungbuk, Korea) for the first dimension, and then sodium dodecyl sulfate polyacrylamide gel electrophoresis (SDS-PAGE; 26×20 cm format) for the second dimension by molecular weight. Proteins were detected by alkaline silver staining.

Quantitative analysis of digitized images was carried out using PDQuest software (version 7.0, BioRad) according to the manufacturer's protocols. Quantity of each spot was normalized by total valid spot intensity.

5. Protein Profile Analysis and Identification by Mass Spectrometry

Clustering of samples and profiling of the protein expression were performed as

described previously.[18] For protein identification, matrix-assisted laser desorption/ionisation-time of flight (MALDI-TOF) mass spectrometer was used as previously described.[18] The obtained amino acid sequence was identified by a homology search using in a BLAST search using the ExPASy Molecular Biology Server (www.expasy.ch).

6. Western blot analysis

To clarify the nuclear shuttling of Nm23-H1, NE-PER® Nuclear and Cytoplasm Extraction Reagents (Pierce Biotechnology, Rockford, IL, USA) were used to separate cytoplasmic and nuclear extracts. Equal amounts of cell extracts were subjected to SDS-PAGE and transferred to a nitrocellulose membrane (Bio-Rad). Anti-Nm23-H1 antibody (1:500 dilution, Abcam, Cambridge, MA, USA) and anti-aurora kinase A (AURKA) antibody (1:500 dilution, Abcam) were used as primary antibodies, and anti-glyceraldehyde-3-phosphate dehydrogenase (1:500 dilution, GAPDH; Santa Cruz Biotechnology, Santa Cruz, CA, USA) was used as the internal control. Next, membranes were washed three times with PBS-T, and incubated for an additional 1 hr with horseradish peroxidase-linked secondary antibody diluted in PBS-T with 5% skimmed milk. Donkey polyclonal antibodies against Nm23-H1, AURKA and rabbit polyclonal antibodies against GAPDH (1:10,000 dilution, Zymed Laboratories Inc, South San Francisco, CA, USA) were used as secondary antibodies.

7. Immunofluorescence

SCC15, SCC25, QLL1, and caki-1 cells seeded on slides were fixed with pre-cooled methanol at -20 °C for 10 min. Cells were incubated with anti-Nm23-H1 (dilution, 1:100 in PBS-T) and then incubated with Alexa Fluor® 594 secondary antibody (dilution, 1:250; Molecular Probes, Eugene, OR, Carlsbad, CA). The slides were washed three times with PBS and mounted with ProLong® Gold Antifade Reagent (Molecular Probes, P36930, Carlsbad, CA, USA). Cells were visualized by fluorescent inverted microscopy (Olympus, IX71 equipped with DP71 camera). Scattergrams were utilized for quantitation of nuclear fractionated frequencies of Nm23-H1. We analyzed all images using TissueQuest software (TissueGnostics, Vienna, Austria) to measure the total cell number from the DAPI images. Cells were plotted according to their Alexa Fluor® 594 intensity vs. their DAPI intensity on the scattergrams. We isolated non-specifically stained structures and large objects from the image.

8. Patients and clinical findings

We found a total of 105 patients who were eligible for this study from patient records of the Yonsei University Health System. All patients had HNSCC (primary tumor staging: T0, 9.5%; T1, 33.3%; T2, 25.7%; T3, 20.0%; T4, 11.4%; and regional lymph node staging: N0, 61.0%; N2, 31.4%) and they were treated with postoperative three-dimensional (3D) conformal radiotherapy for the past 10 years (mean age ± standard deviation [SD], 58.2 ± 11.7 years; male, $n = 81$ [77.1%]).

Mean overall survival time was 696.3 months (median, 565.5 months). Mean recurrence-free survival was 569.1 months (median, 426.0 months). All patients provided written informed consent, and the study was approved by the Research Ethics Board of Yonsei University Health System.

All patients underwent computed tomography (CT) simulation (Picker PQ5000 CT scanner, Phillips Medical Systems, Andover, MA, USA) with 5-mm thick slice cuts. Intravenous contrast agents were used in all patients. Structures were manually contoured onto the CT scan slices following the recommendations of the International Commission on Radiation Units and Measurements Report 50.

All patients received 3D conformal radiotherapy with single daily fractions of 2.0 Gy, 5 days per week. The planned total dose was 60 to 70.0 Gy over 6 to 7 weeks. The radiation treatment areas included the gross primary tumor as well as the regional neck nodes. Radiotherapy was performed with 4-MV photon beams from a linear accelerator (CLINAC 600C, Varian Medical Systems, Palo Alto, CA, USA). Field reduction at 44 or 45 Gy was completed to exclude the spinal cord from the large fields. The remaining dose was delivered to smaller lateral or oblique fields, including only the primary tumor and clinically or radiographically detectable nodes with a margin of 1 cm. Electron beams of suitable energy were used to boost the primary tumor site as well as grossly involved lymph nodes.

9. Immunohistochemistry

The 4-μm tissue sections were placed on silane-coated slides, deparaffinized,

immersed in PBS containing 0.3% (v/v) hydrogen peroxide, and then were processed in a microwave oven (in 10 mM sodium citrate buffer, pH 6.5, for 15 min at 700 W). After blocking with 1% (w/v) bovine serum albumin in PBS containing 0.05% (v/v) Tween-20 for 30 min, the sections were incubated with biotin-labeled rabbit anti-Nm23-H1 polyclonal antibodies (dilution, 1:2,000; Abcam) and with biotin-labeled rabbit anti-AURKA polyclonal antibodies (dilution, 1:400; Abcam) at 4°C for 16h, respectively. Biotinylation of the antibodies was performed with an antibody biotin-labeling kit (Dako, Envision, Glustrup, Denmark). Streptavidin-conjugated peroxidase was used as a secondary antibody (1:10,000). Normal goat serum and subtype-matched normal mouse IgG were used as negative controls. The final reaction product was visualized by adding 0.03% (w/v) of 3, 3′-diaminobenzidine tetrachloride (DAB) for 5 to 20 min. Carcinomas were semi-quantified using a two-tier system (0: negative staining, 1: weakly focal positive less than 50%, 2: strong positive more than 50%) which included immunolocalization of cytoplasm and/or nucleoplasm.

10. Statistical analysis

Patients were categorized according to Nm23-H1 expression and localization. Time to recurrence was measured from the date of diagnosis to the date of the first local or distant metastasis or to the last follow-up. Patients who died before disease recurrence were considered censored at the date of death. Patients who experienced local recurrence as the first recurrence were considered censored at the date of local

recurrence. Times to local and distant recurrence were estimated by Kaplan-Meier analysis, and comparisons between groups were made with log-rank statistics. Cox proportional hazards models were used to determine the association between expression and nuclear localization of Nm23H1 and the risk of RR as assessed by local recurrence. Each model contained terms for Nm23-H1 cytoplasmic expression, Nm23-H1 nuclear localization, age at diagnosis, tumor size, tumor type, histological grade, T-stage, N-stage, M-stage, and incomplete margin. *P* less than 0.05 was considered significant. Statistical analyses were performed using SAS software (SAS, Cary, NC, USA).

III. RESULTS

1. Screening of radiation resistance-related genes by cDNA array and proteomics

A total of 533 genes were differentially expressed in the cDNA array; 265 genes were upregulated and 268 genes were downregulated in RR-60 cell lines compared to non-irradiated cells. One-way hierarchical clustering showed both upregulated and downregulated genes (Fig. 1A).

Fifty-seven proteins ($p<0.05$) were screened by MALDI-TOF. In analysis of the distance map tree, the distance between non-irradiated and irradiated cell lines of RR-60 (SCC15, SCC25, and QLL1) was significantly great (Fig. 1B).

In cDNA array data, DNA repair gene (RFC4), cell cycle-related gene (CCND1), or signal transduction related genes (FZD5, CTNNA1) were significantly altered with more than 2-fold expression. In addition, cell death or senescence related genes (i.e.,AATF, TNFRSF11B, DDX60L, or MAPK6) were significantly related. In proteomics data, most proteins related to cell cycle-related proliferation (EIF2S2, PA2G4, MET, MCM4), DNA replication (WDR77) were upregulated, while GSTM3 was downregulated. Notably, Nm23-H1 was the only overlapping gene product which was detected in both cDNA array and proteomics (Fig. 1C).

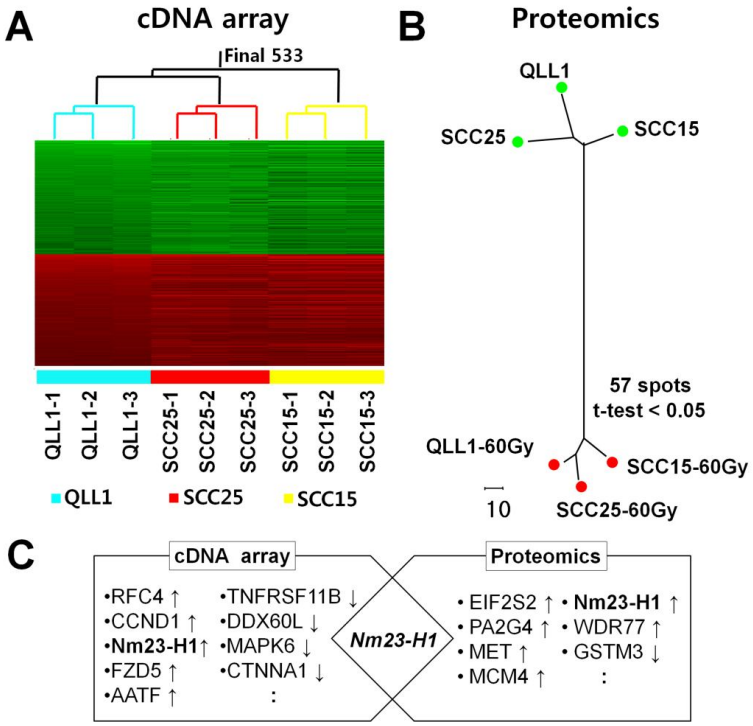

FIGURE 1. Screening of radiation resistance predictors by cDNA array and proteomics using three different head and neck squamous cell carcinoma cell lines: SCC15, SCC25, and QLL1. (A) Hierarchical clustering of cDNA array. The clustering of SCC15 differed from those of SCC25 and QLL1. (B) Distance map tree represents relative distances between non-irradiated cells and RR-60 cells from a total of 57 spots ($P < 0.05$). (C) Overexpression of Nm23-H1 is observed in both cDNA array and proteomics results.

2. Validation of Nm23-H1 detected by cDNA array and proteomics

Both cDNA array and proteomics results showed Nm23-H1 as the strongest predictor of RR. The Nm23-H1 spot significantly increased in RR-60 SCC15 and

SCC25, but not in QLL1. Relative intensities represent the spot densities on the 2D gel. Nearly a two-fold higher density was observed in RR-60 SCC15 and SCC25 (Fig . 2A). The immunoblotting results revealed that Nm23-H1 was similarly overexpressed as in the proteomics results but downregulated in QLL1 cells (Fig. 2B).

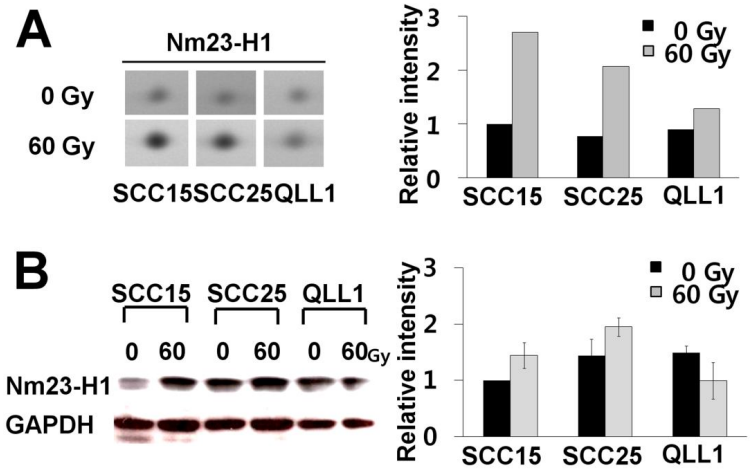

FIGURE 2. Validation of Nm23-H1. (A) Proteomics spots were identified as Nm23-H1. Irradiated SCC15 and SCC25 cell lines showed increased spot density. (B) In western blotting, SCC15 and SCC25 cells showed high levels of Nm23-H1 expression in RR-60 cells, while the expression was low in QLL1 cells after GAPDH normalization.

3. In vitro nuclear translocation of Nm23-H1 by indirect immunofluorescence

Immunofluorescence demonstrated that Nm23-H1 is generally localized in the cytoplasm in non-irradiated HNSCC cell lines. However, HNSCC cells that

received a 4 Gy dose of fractionated radiation (RR-4) demonstrated nuclear localization of Nm23-H1. Nm23-H1 was rarely observed in the nuclei of HNSCC and caki-1 cells that were not irradiated. Caki-1 cells showed nuclear localization of Nm23-H1 in dot patterns after a 4 Gy dose of irradiation. Both RR-4 and RR-60+4 demonstrated fewer nuclear signals than RR-60, but were intensively stained (Fig. 3A). Nuclear fluorescent signals were quantified by scattergram. The proportion of Nm23-H1 nuclear fluorescent signals was increased in RR-60 when compared to non-irradiated cell lines (Fig. 3B). After nuclei/cytoplasm fractionation, Nm23-H1 signal was elevated after a single dose of 4 Gy irradiation in non-irradiated cells. However, RR-60 cells after a 4 Gy booster dose of irradiation did not induce overexpression of Nm23-H1. AURKA expression showed a similar pattern with Nm23-H1. Nm23-H1 expression level in RR-60 of QLL1 was the same with western blotting as shown in Fig.2B. For this reason, the relationship between AURKA and Nm23-H1 in RR-60 cells of QLL1 was quite different from other cell lines. The relative intensity of the right panel represents the quantity of Nm23-H1 and AURKA in nucleus after GAPDH normalization (Fig. 3C).

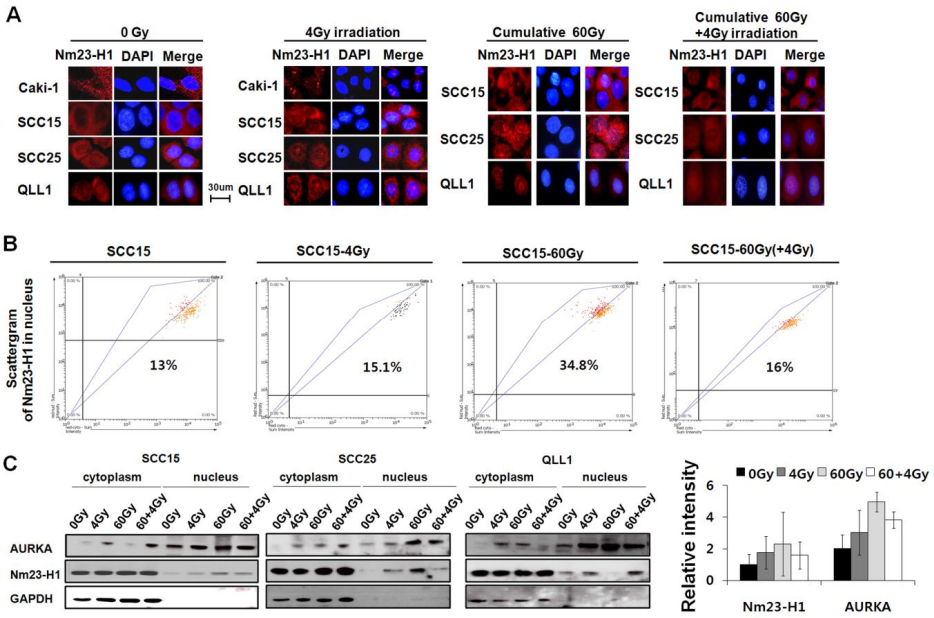

FIGURE 3. Nm23-H1 nuclear translocation in radiation-treated cell lines. Nm23-H1 translocated to the nucleus in head and neck cancer cell lines, SCC15, SCC25, and QLL1, with a 4 Gy (human LD_{50}) radiation treatment in non-irradiated cells. (A) Each panel indicates the localization and intensity of Nm23-H1. The first panel shows non-irradiated cells. Cells in the next panel were treated with a single 4 Gy dose of radiation. The third panel displays RR-60 cell lines, and the last panel indicates a radiation-resistant cell line (treated with a total dose of 60 Gy) after a booster dose of 4 Gy. Notice the nuclear speckled pattern in the caki-1 cell line after a 4 Gy dose of irradiation. (B**)** Quantitative analysis of immunofluorescene stainning of Nm23-H1. Each scattergram represents the nucleoplasm intensity in SCC15 cell line in a radiation dose dependent manner. **(C)** The expression quantity of Nm23-H1 and AURKA in the nucleoplasm was estimated by western blotting,

and the highest expression was observed in RR-60 cells. The right panel represents the relative intensity of Nm23-H1 and AURKA after GAPDH normalization.

4. Immunohistochemistry of Nm23-H1 and AURKA in clinical samples with RR

The most common finding of Nm23-H1 in HNSCC cells was intense staining, especially of tumor nests, in contrast to no Nm23-H1 staining in normal squamous epithelium (NL) (Fig. 4A). After the analysis of 105 tissue samples, only cytoplasmic Nm23-H1 expression was detected in 94 samples (89.52%). Additional nuclear expression was detected in 21 samples (20%) with five samples showing predominantly nuclear localization. Nm23-H1 distribution was accentuated along the tumor margin (Fig 4B). Diffusely infiltrative cancer cells accompanied by a desmoplastic stromal reaction showed remarkably strong nuclear staining compared with relatively weak staining in the epicenters of tumor nests (Fig. 4C). A patch-like distribution of Nm23-H1 was apparent along the invasive front of the tumor (Fig. 4D). Nm23-H1 was diffusely localized within the nuclei of certain RR tissues (Fig. 4E) in addition to a typical cytoplasmic expression (Fig. 4F). AURKA showed nuclear expression in all cancer cells**,** more intensely in invasive cells, in particular (Fig. 4G). All with Nm23-H1 nuclear expression demonstrated AURKA nuclear coexpression.

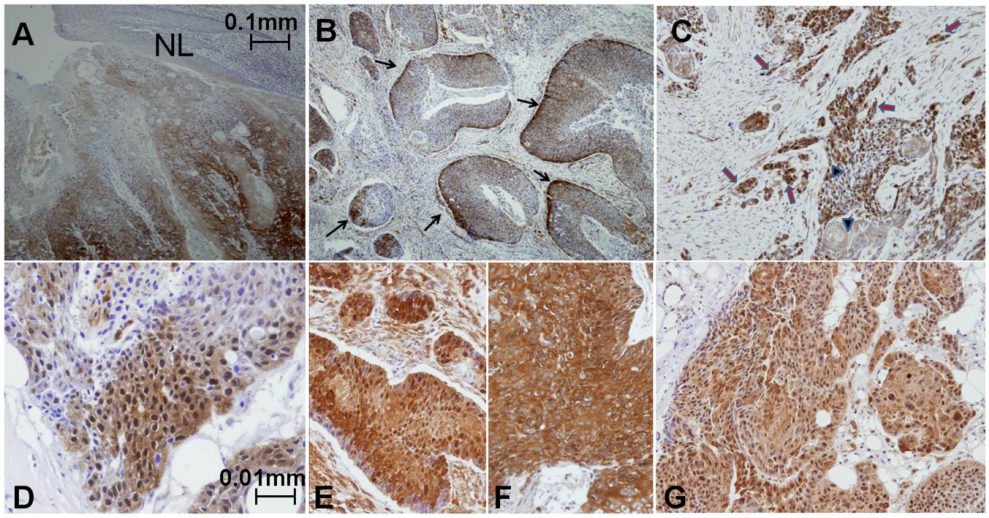

FIGURE 4. Immunohistochemistry of Nm23-H1 in HNSCC archival tissue samples from patients who presented with locoregional failure after therapeutic radiotherapy. (A) Typical expression of Nm23-H1 along the basal layers and invasive squamous cell carcinoma (SCC). Notice the negative staining in the normal squamous epithelium (NL). (B) Nm23-H1 revealed strong immunoreactivity along the margin of invasive tumor nests (arrows). (C) Remarkable nuclear staining in infiltrative tumor nests within the desmoplastic stromal reaction (arrow). Note the relatively weak staining in the epicenters of SCC nests (arrowhead). (D) A patch-like distribution of Nm23-H1 nuclear staining in invasive fronts of the tumor. (E) Diffuse nuclear localization of Nm23-H1. (F) Cytoplasmic staining of Nm23-H1 with no obvious nuclear localization identified in most tumor nests. (G) AURKA showed nuclear expression in all cancer cells, more intensely in the invasive cells in particular.

5. Association of Nm23-H1 expression with overall or recurrence-free survival

Kaplan-Meier analysis demonstrated a significant association between cytoplasmic/nuclear expression of Nm23-H1 and overall/recurrence-free survival (Fig. 5). Analysis of overall and recurrence-free survival using Cox proportional hazard model is displayed in Tables 1 and 2, respectively. Nuclear localization and cytoplasmic expression of Nm23-H1 as well as cancer T stage were strongly associated with overall survival in the univariate model, whereas Nm23-H1 nuclear localization (7.48 OR) and N stage (2.13 OR) were significant factors in the multivariate Cox hazard model (Table 1). In terms of recurrence-free survival, cytoplasmic and nuclear expressions of Nm23-H1 as well as insufficient tumor margins were significant in univariate analysis, and Nm23-H1 nuclear localization (OR, 2.38) and indeterminate margin (OR, 3.81) were confirmed by multivariate stepwise Cox regression analysis (Table 2).

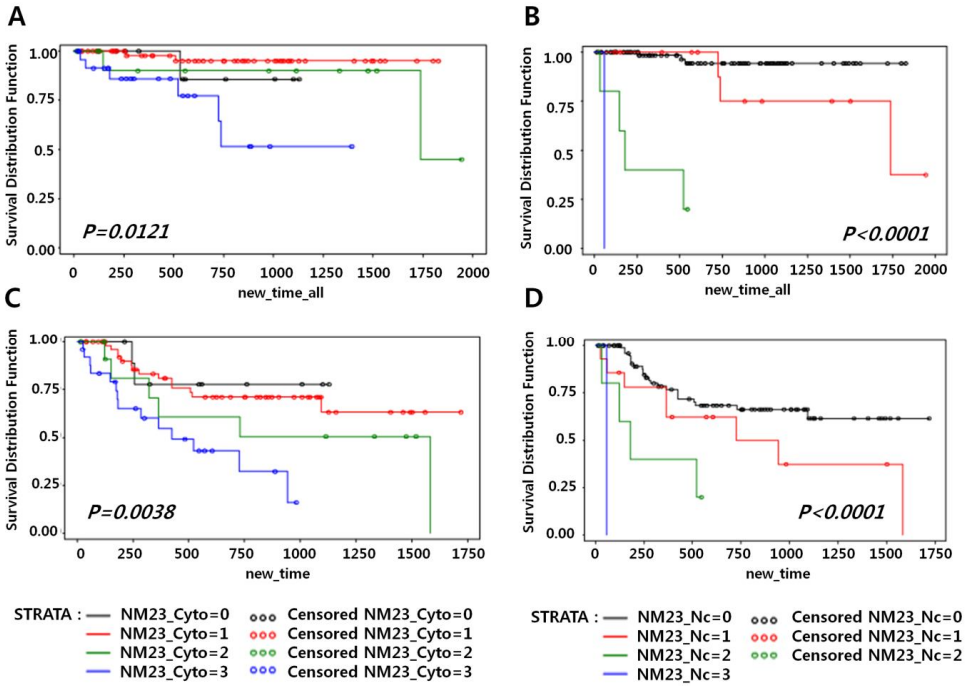

FIGURE 5. Kaplan-Meier analysis of Nm23-H1 expression and survival. **(**A) Association between Nm23-H1 cytoplasmic expression and overall survival. (B) Association between Nm23-H1 nuclear expression and overall survival. (C) Association between Nm23-H1 cytoplasmic expression and recurrence-free survival. (D) Association between Nm23-H1 nuclear expression and recurrence-free survival.

Table 1. Univariate and multivariate overall survival analyses using the Cox proportional hazard model.

Characteristic	Univariate		Multivariate	
	P	**HR**	***P***	**HR**
Age	0.5572	0.99	0.1486	1.07

Tumor margin	0.0695	2.16	0.3265	3.30
Tumor size	0.1333	1.14	0.8746	1.07
Nm23-Cyto	**0.0064**	**2.54**	0.2340	0.54
Nm23-Nuc	**<0.0001**	**7.54**	**<0.0001**	**7.48**
T stage	**0.0366**	**1.35**	0.8138	1.14
N stage	0.1925	1.25	**0.0254**	**2.13**

HR indicates hazard ratio; Nm23-Cyto, cytoplasmic localization of Nm23-H1; Nm23-Nuc, nuclear localization of Nm23-H1.

Table 2. Univariate and multivariate recurrence-free survival analyses using the Cox proportional hazard model.

Characteristic	**Univariate**		**Multivariate**	
	P	**HR**	***P***	**HR**
Age	0.4925	0.99	0.4221	0.99
Tumor margin	**0.0113**	**3.17**	**0.0037**	**3.81**
Tumor size	0.8764	0.97	0.8320	0.96
Nm23-Cyto	**0.0009**	**1.78**	0.1617	1.39
Nm23-Nuc	**0.0001**	**2.40**	**0.0138**	**2.38**
T stage	0.1315	1.47	0.0812	1.61
N stage	0.8953	0.97	0.8331	0.96

HR indicates hazard ratio; Nm23-Cyto, cytoplasmic localization of Nm23-H1; Nm23-Nuc, nuclear localization of Nm23-H1.

IV. DISCUSSION

Although many tried to uncover biomarkers that predict RR in HNSCC, only Akt phosphorylation, overexpression of HIF1a and carbonic anhydrase 9,[7, 8] and ERCC1[9] were found. Those studies were only involved in immunochemical analysis of tissues from patients with locoregional failure which have limitation in apply for diagnosis. To find more reliable markers for RR, we established RR-60 cell lines by exposing a cumulative dose of 60 Gy and compared with non irradiated cell lines using both preliminary transcriptomics and proteomics screeining. The 60 Gy dose of irradiation is a widely used dosage in HNSCC radiotherapy as well as investigation on tissue samples.

There were several studies using cDNA array or proteomics to discover markers for RR in HNSCC.[19, 20] One study found that the expression of 25 genes were altered by radiation and 11 of them were validated in oral squamous cell carcinoma cell lines after radiation up to 8 Gy such as ICAM2, TIMP3, PLAGL1, and FGFR3.[20] In another study, 48 genes were significantly altered in myeloid cell lines (ML-1) by radiation which were primarily apoptosis-related genes such as Fas, Ciap1, Bak, and Bcl-XL.[21] In a study using proteomics, head and neck cancer cell lines which were exposed to 4 Gy dose of radiation showed differential expression of proteins as follows: heat shock protein (hsp) 27, peroxiredoxin (Prx) II, and glutathione S-transferase pi (GSTP).[22] Although many putative RR-related genes or proteins have been found, the demand for reliable RR marker is still remained. In our study, we used both cDNA array and proteomics for screening, which may

increase the reliability of RR-candidates by being double-checked, in RR-60 and non-irradiated cell lines.

Nm23-H1 was significantly increased in RR-60 cell lines and non-irradiated cells exposed to 4 Gy of booster irradiation. And also the overexpression of Nm23-H1 in nucleus was found in RR-60 cell lines. It has been reported that Nm23-H1 is usually located in cytoplasm, not nucleus. Therefore, we postulated that Nm23-H1 would have another function on RR by nuclear translocation. To determine how cells respond to radiation, especially in Nm23-H1 expression in nucleus, we exposed each cell lines to 4 Gy booster radiation. The overexpression of Nm23-H1 in nucleus was observed in the non-irradiated cell lines exposed to 4 Gy of booster irradiation. However, there was no significant increase of Nm23-H1 in nucleus of RR-60 cell lines. RR-60 cells may have already acquired Nm23-H1 overexpression in nucleus by repeated radiation. The assumption can be supported by the report that Nm23-H1 may play a role in DNA damage repair or the induction of DNA synthesis.[23, 24] Nm23-H1-mediated DNA repair maintains genomic stability after irradiation or UV irradiation.[23, 24] DNA repair from irradiation targeted to dsDNA of cancer cells may lead to survival of cancer.

In addition, we validated predictor (Nm23-H1) expression in a large number of tissues from HNSCC patients with locoregional failure. As we mentioned above, Nm23-H1 is normally found in cytoplasm, and its nuclear localization has seldom been reported. However, we observed nuclear localization of Nm23-H1 in HNSCC. The most common finding of Nm23-H1 was cytoplasmic staining with accentuation

along the tumor margins or invasive fronts, but nuclear and cytoplasmic coexpression was also detected in 20% of a total samples. We noticed the findings of accentuation along the tumor margins or invasive fronts of Nm23-H1, which represent Nm23-H1 has to do with invasive potential and poor prognostic factor. In addition to distribution patterns, multivariate Cox hazard model also showed nuclear localization as a significant poor prognostic factor. Our finding is consistent with another study reporting Nm23-H1 nuclear localization as a progressive marker in breast cancer.[25] Both nuclear and cytoplasmic staining were in 24.3% of node-positive infiltrating ductal carcinoma (IDC) and 18.9% of matched node metastasis cases compared with 4.9% staining in node-negative IDC.[25]

The functional mechanism of Nm23-H1 nuclear translocation as a poor prognostic factor has not been clarified. With specific regards to the functional mechanism, Fan et al mentioned that Granzyme A secreted from cytotoxic T cell can induce the single strand DNA nick of target cells via the nuclear translocation of Nm23-H1.[26] In another report, Nm23-H1 interacts with AURKA which might function in radioresistance.[27, 28] AURKA is a centrosome-associated kinase and its overexpression in rodent and human cancer cells causes improper centrosome duplication, aneuploidy and cellular transformation.[27] Accumulation of Nm23-H1 on the centrosome coincides with the enrichment of AURKA at the centrosome and with increased AURKA activity in the beginning of mitosis through the microtubule-independent mechanism.[28] Based on references and our results, Nm23-

H1 may play a role in DNA damage repair or the induction of DNA synthesis together with AURKA. AURKA showed coexpression pattern with Nm23-H1 in SCC15, SCC25 but not in QLL1. AURKA showed nuclear expression in all cancer cell lines and its expression pattern was overlapped with Nm23-H1 in most cases. According to coexpression with AURKA in the event of nuclear translocation of Nm23-H1, we suggest another putative pathway by which Nm23-H1 directly interacts with AURKA in head and neck cancer undergoing RR.

V. CONCLUSION

Nm23-H1 is a reliable candidate for RR prediction in HNSCC. There has not been any report on Nm23-H1 overexpression in nuclus and nuclear translocation in other cancers such as thyroid cancer, ovarian cancer, T-cell lymphoma, and neuroblastomas after irradiation.[29-32] And also there are several reports that Nm23-H1 expression is associated with a favorable prognosis or shows a lack of association with head and neck cancer.[33, 34]. Thus, Nm23-H1 is thought to have tissue-specific roles with different regulatory mechanisms and its overexpression may be specific to HNSCC.

In conclusion, nuclear translocation of Nm23-H1 may be a meaningful and strong predictor of RR in patients with HNSCC.

References

1. Hardisson D. Molecular pathogenesis of head and neck squamous cell carcinoma. Eur Arch Otorhinolaryngol 2003;260:502-8.
2. Le Tourneau C, Siu LL. Molecular-targeted therapies in the treatment of squamous cell carcinomas of the head and neck. Curr Opin Oncol 2008;20:256-63.
3. Dassonville O, Formento JL, Francoual M, Ramaioli A, Santini J, Schneider M, et al. Expression of epidermal growth factor receptor and survival in upper aerodigestive tract cancer. J Clin Oncol 1993;11:1873-8.
4. Wen QH, Miwa T, Yoshizaki T, Nagayama I, Furukawa M, Nishijima H. Prognostic value of EGFR and TGF-alpha in early laryngeal cancer treated with radiotherapy. Laryngoscope 1996;106:884-8.
5. Thariat J, Yildirim G, Mason KA, Garden AS, Milas L, Ang KK. Combination of radiotherapy with EGFR antagonists for head and neck carcinoma. Int J Clin Oncol 2007;12:99-110.
6. Gallo O, Chiarelli I, Boddi V, Bocciolini C, Bruschini L, Porfirio B. Cumulative prognostic value of p53 mutations and bcl-2 protein expression in head-and-neck cancer treated by radiotherapy. Int J Cancer 1999;84:573-9.
7. Gupta AK, McKenna WG, Weber CN, Feldman MD, Goldsmith JD, Mick R, et al. Local recurrence in head and neck cancer: relationship to radiation resistance and signal transduction. Clin Cancer Res 2002;8:885-92.
8. Koukourakis MI, Giatromanolaki A, Danielidis V, Sivridis E. Hypoxia inducible

factor (HIf1alpha and HIF2alpha) and carbonic anhydrase 9 (CA9) expression and response of head-neck cancer to hypofractionated and accelerated radiotherapy. Int J Radiat Biol 2008;84:47-52.

9. Kim MK, Cho KJ, Kwon GY, Park SI, Kim YH, Kim JH, et al. ERCC1 predicting chemoradiation resistance and poor outcome in oesophageal cancer. Eur J Cancer 2008;44:54-60.
10. Sims-Mourtada J, Izzo JG, Apisarnthanarax S, Wu TT, Malhotra U, Luthra R, et al. Hedgehog: an attribute to tumor regrowth after chemoradiotherapy and a target to improve radiation response. Clin Cancer Res 2006;12:6565-72.
11. Lascu L. The nucleoside diphosphate kinases 1973-2000. J Bioenerg Biomembr 2000;32:213-4.
12. Kantor JD, McCormick B, Steeg PS, Zetter BR. Inhibition of cell motility after nm23 transfection of human and murine tumor cells. Cancer Res 1993;53:1971-3.
13. Hartsough MT, Morrison DK, Salerno M, Palmieri D, Ouatas T, Mair M, et al. Nm23-H1 metastasis suppressor phosphorylation of kinase suppressor of Ras via a histidine protein kinase pathway. J Biol Chem 2002;277:32389-99.
14. Salerno M, Palmieri D, Bouadis A, Halverson D, Steeg PS. Nm23-H1 metastasis suppressor expression level influences the binding properties, stability, and function of the kinase suppressor of Ras1 (KSR1) Erk scaffold in breast carcinoma cells. Mol Cell Biol 2005;25:1379-88.
15. Eckes B, Dogic D, Colucci-Guyon E, Wang N, Maniotis A, Ingber D, et al. Impaired mechanical stability, migration and contractile capacity in vimentin-

deficient fibroblasts. J Cell Sci 1998;111:1897-907.

16. Otero AS. Copurification of vimentin, energy metabolism enzymes, and a MER5 homolog with nucleoside diphosphate kinase. Identification of tissue-specific interactions. J Biol Chem 1997;272:14690-4.

17. Ki DH, Jeung HC, Park CH, Kang SH, Lee GY, Lee WS, et al. Whole genome analysis for liver metastasis gene signatures in colorectal cancer. Int J Cancer 2007;121:2005-12.

18. Kim DS, Choi YP, Kang S, Gao MQ, Kim B, Park HR, et al. Panel of candidate biomarkers for renal cell carcinoma. J Proteome Res 2010;9:3710-9.

19. Frederick BA, Helfrich BA, Coldren CD, Zheng D, Chan D, Bunn PA Jr, et al. Epithelial to mesenchymal transition predicts gefitinib resistance in cell lines of head and neck squamous cell carcinoma and non-small cell lung carcinoma. Mol Cancer Ther 2007;6:1683-91.

20. Ishigami T, Uzawa K, Higo M, Nomura H, Saito K, Kato Y, et al. Genes and molecular pathways related to radioresistance of oral squamous cell carcinoma cells. Int J Cancer 2007;120:2262-70.

21. Amundson SA, Bittner M, Chen Y, Trent J, Meltzer P, Fornace AJ Jr. Fluorescent cDNA microarray hybridization reveals complexity and heterogeneity of cellular genotoxic stress responses. Oncogene 1999;18:3666-72.

22. Lee YS, Chang HW, Jeong JE, Lee SW, Kim SY. Proteomic analysis of two head and neck cancer cell lines presenting different radiation sensitivity. Acta Otolaryngol 2008;128:86-92.

23. Kaetzel DM, Zhang Q, Yang M, McCorkle JR, Ma D, Craven RJ. Potential roles of 3'-5' exonuclease activity of NM23-H1 in DNA repair and malignant progression. J Bioenerg Biomembr 2006;38:163-7.

24. Yang M, Jarrett SG, Craven R, Kaetzel DM. YNK1, the yeast homolog of human metastasis suppressor NM23, is required for repair of UV radiation- and etoposide-induced DNA damage. Mutat Res 2009;660:74-8.

25. Ismail NI, Kaur G, Hashim H, Hassan MS. Nuclear localization and intensity of staining of nm23 protein is useful marker for breast cancer progression. Cancer Cell Int 2008;8:6.

26. Fan Z, Beresford PJ, Oh DY, Zhang D, Lieberman J. Tumor suppressor NM23-H1 is a granzyme A-activated DNase during CTL-mediated apoptosis, and the nucleosome assembly protein SET is its inhibitor. Cell 2003;112:659-72.

27. Guan Z, Wang XR, Zhu XF, Huang XF, Xu J, Wang LH, et al. Aurora-A, a negative prognostic marker, increases migration and decreases radiosensitivity in cancer cells. Cancer Res 2007;67:10436-44.

28. Du J, Hannon GJ. The centrosomal kinase Aurora-A/STK15 interacts with a putative tumor suppressor NM23-H1. Nucleic Acids Res 2002;30:5465-75.

29. An HJ, Kim DS, Park YK, Kim SK, Choi YP, Kang S, et al. Comparative proteomics of ovarian epithelial tumors. J Proteome Res 2006;5:1082-90.

30. Niitsu N, Nakamine H, Okamoto M, Akamatsu H, Honma Y, Higashihara M, et al. Expression of nm23-H1 is associated with poor prognosis in peripheral T-cell lymphoma. Br J Haematol 2003;123:621-30.

31. Takeda O, Handa M, Uehara T, Maseki N, Sakashita A, Sakurai M, et al. An increased NM23H1 copy number may be a poor prognostic factor independent of LOH on 1p in neuroblastomas. Br J Cancer 1996;74:1620-6.

32. Zou M, Shi Y, al-Sedairy S, Farid NR. High levels of Nm23 gene expression in advanced stage of thyroid carcinomas. Br J Cancer 1993;68:385-8.

33. Gunduz M, Ayhan A, Gullu I, Onerci M, Hosal AS, Gursel B, et al. nm23 Protein expression in larynx cancer and the relationship with metastasis. Eur J Cancer 1997;33:2338-41.

34. Wang YF, Chow KC, Chang SY, Chiu JH, Tai SK, Li WY, et al. Prognostic significance of nm23-H1 expression in oral squamous cell carcinoma. Br J Cancer 2004;90:2186-93.

ABSTRACT (IN KOREAN)

두경부 편평세포암에서

Nm23-H1 단백질의 핵으로의 이동과 방사선 저항과의 연관성

<지도교수 조 남 훈>

연세대학교 대학원 의과학과

박 행 란

실험 배경 : 방사선 치료에 있어서 방사선 저항은 근본적인 문제점이고, 이를 극복하기 위한 예측 마커를 찾는 많은 시도들이 있어 왔지만, 확실한 지표를 찾는데 실패하였다. 따라서, 저자는 두경부편평세포암에서 진단 예측을 증진시킬 수 있는 방사선 내성 예측 지표를 연구하고자 하였다.

실험 방법 : SCC15, SCC25 와 QLL1 의 두경부편평세포암 세포주에 각각 4Gy, 누적 방사선량 60Gy(방사선 내성 세포주), 누적 방사선량 60Gy에 추가 4Gy를 준 후, 대조실험군과의 차이점을 cDNA array, 프로테오믹스, 웨스턴 블롯팅 및 면역형광염색 방법을 이용하여 연구하였다. 방사선 내성을 보였던 105 개의 두경부편평세포암 환자의 조직 샘플을 면역조직염색을 통해 분석하였다.

실험 결과 : cDNA array 및 프로테오믹스로 방사선 내성 세포주에서 특이적 발현 변화를 보인 유전인자를 선별한 결과 Nm23-H1 단백질이 방사선 내성 세포주에서 과발현이 확인되었고, 이의 유효화 실험인 웨스턴 블롯팅에서도 같은 결과를 얻었다. 세포내에서의 Nm23-H1의 발현 위치를

보기 위해 면역형광염색을 시행하였고, 그 결과 4Gy의 방사선을 받은 세포 및 방사선 내성 세포에서 대조실험군에서 보이지 않았던 Nm23-H1 단백질의 핵내로의 이동을 관찰하였고, 방사선 내성 세포주에 추가 4Gy의 방사선을 준 세포에서도 관찰이 되었다. 이와 유사하게, Nm23-H1에 대한 면역 조직 염색 결과 방사선 내성을 보인 환자 조직 중 약 20%에서 핵내 관찰이 확인 되었다.일변량 분석 결과는 Nm23-H1 단백질의 핵내 관찰은 전체 생존율 및 무재발 생존율과 상당한 연관이 있다고 나타냈다.다변량 단계별 Cox 회귀 분석 결과 Nm23-H1 단백질의 핵내 관찰과 종양의 림프절 전이 여부는 전체 생존률과 관련 있다고 나타났고, Nm23-H1과 원발병소의 크기 및 종양 가장자리는 무재발 생존율과 연과되어 있다고 나타났다.

결론 : Nm23-H1 단백질의 과발현, 특히 핵내 이동은 두경부편평세포암에서 방사선 저항을 예측할 수 있는 예측지표가 될 수 있을 것이다.

핵심되는 말 : Nm23-H1, 핵 내 이동, 방사선 저항, 두경부 편평세포암, 예측 지표